ISSN 1075-7015, Geology of Ore Deposits, 2016, Vol. 58, No. 4, pp. 327–343. © Pleiades Publishing, Ltd., 2016.
Original Russian Text © V.B. Naumov, A.V. Girnis, V.A. Dorofeeva, V.A. Kovalenker, 2016, published in Geologiya Rudnykh Mestorozhdenii, 2016, Vol. 58, No. 4, pp. 367–384.

Concentration of Ore Elements in Magmatic Melts and Natural Fluids as Deduced from Data on Inclusions in Minerals

V. B. Naumov[a], **A. V. Girnis**[b], **V. A. Dorofeeva**[a], **and V. A. Kovalenker**[b]

[a] *Vernadsky Institute of Geochemistry and Analytical Chemistry,*
Russian Academy of Sciences, ul. Kosygina 19, Moscow, 119991 Russia
[b] *Institute of Geology of Ore Deposits, Petrography, Mineralogy, and Geochemistry,*
Russian Academy of Sciences, Staromonetnyi per. 35, Moscow, 119017 Russia

Received July 10, 2015

Abstract—Based on intergration of the published data on composition of inclusions in minerals and quenched glasses, the mean concentrations of 24 ore elements have been calculated for magmatic silicate melts formed in main geodynamic settings of the Earth and in natural fluids. The mean glass compositions normalized to the primitive mantle correlate with the partition coefficient between olivine and the basic melt. It is established that the degree of enrichment in ore elements depending on geodynamic setting is controlled by various contribution of fluids to the element transfer and accumulation. The ratios of element contents in each geodynamic setting to the mean concentrations of elements over all settings in the Earth have been calculated.

DOI: 10.1134/S1075701516040048

INTRODUCTION

The neverending interest in magmatic (related to a particular degree to magmatism) deposits is determined by their crucial significance as a source of noble, nonferrous, and rare metals. The study of these deposits is primarily aimed at elucidating their formation in various geodynamic settings, creating descriptive and genetic models for forecasting, prospecting, and assessing territories with respect to economically important mineral deposits (Hedenquist and Lowenstern, 1994; Kerrich et al., 2000; Sillitoe, 2000, 2010; Lang and Baker, 2001; Meinert et al., 2003; Richards, 2003; Seedorff et al., 2005; Sillitoe and Hedenquist, 2003; Kovalenker, 2006; Safonov et al., 2006; Bortnikov et al, 2012; Volkov et al., 2014; Mao *et al.*, 2014).

These and other related publications consider the key problems of ore geology and metallogeny in regards to the structure of the lithosphere, petrology, and tectonic regimes of continental crust formation with case studies of the main types of deposits associated with intrusions. The physicochemical processes responsible for the formation of magmas enriched in metals, volatile components, and water are also involved in the discussion.

The complexity and diversity of the origin of magmatic deposits and sources of metals and fluids necessary for their formation are underscored by the specific geochemical profile of mineralization: Ni, Cu, Cr, Co, and PGE deposits are associated with mafic and ultramafic igneous bodies; Cu, Au, Ag, Mo, W, and Sn deposits are related to intermediate and felsic magmas; deposits with rare elements, including REE, are derivatives of alkaline melts.

Broadly speaking, this implies that in many cases regional metallogenic features are determined by the occurrence of certain igneous rocks specific in chemical composition. The close genetic links between subduction-related calc-alkaline magmas and porphyry-type Cu, Au, Mo and epithermal Au, Ag, Cu, Pb, Zn deposits at active continental margins and in island arcs are a striking example (Hedenquist and Lowenstern, 1994; Sawkins, 1990). Another example is the obvious association of world-class porphyry and epithermal Au, Cu, Te deposits, including a high percentage of large and superlarge objects, with high-K alkaline magmas (Sillitoe, 1997; Müller and Forrestal, 1998; Zhao et al., 2003). The specificity of these alkaline rocks, which occupy no more than 5–10 vol % in island-arcs and at active margins, consists in low sulfur concentrations, but there are high fO_2 and high concentrations of the volatile component; 40% of the largest epithermal and porphyry Au–Cu deposits worldwideare associated with these rocks (Zhao *et al.*, 2003).

As concerns the source of metals, some authors suggest that a subducted oceanic plate (slab) or overlying metasomatized mantle wedge could be such sources for the deposits associated with felsic magmatism in volcanic–plutonic arcs (Sillitoe, 1997; Mungall, 2002). Others involve anatexis of the lower crust

---

Corresponding author: A.V. Girnis. E-mail: girnis@igem.ru

Table 1. Number of publications containing data on concentrations of ore elements (V, Cr, Co, Ni, Cu, Zn, Ga, Ge, As, Nb, Mo, Ag, Cd, In, Sn, Sb, Ta, W, Au, Tl, Pb, Bi, Th, U) in magmatic silicate melts and natural fluids, which appeared in print in different time periods

Period	Number of publications	
	melts	fluids
1975–1979	1	–
1980–1984	5	–
1985–1989	20	–
1990–1994	40	4
1995–1999	80	6
2000–2004	134	25
2005–2009	154	50
2010–2014	174	66
1975–2014	608	151

(Hedenquist and Lowenstern, 1994; Tomkins and Mavrogenes, 2003) or residual mantle heterogeneity (Sillitoe, 1972). It is also supposed that formation of ore-producing magmas is related to mixing of mantle and crustal materials (Richards, 2003).

In contrast, gold mineral-forming systems (so-called intrusion-related and granite-related deposits) are commonly associated with reduced magmatic melts, which are likely products of partial melting of crustal rocks (Lang and Baker, 2001). This casts doubt on the need for an oceanic plate or mantle to be a source of gold (Tomkins et al., 2009). Therefore, it is important to reveal the processes that influence the metal contents in these crustal rocks.

Up to now, a great deal of data has been published on concentrations of ore elements and volatile components (H_2O, Cl, S) in natural silicate melts formed in various geodynamic settings. These studies became especially efficient with the implementation of local quantitative analysis (electron, ion, and proton microprobes; Raman spectroscopy, mass spectrometry with laser ablation; local infrared spectroscopy, etc.). In this paper, based on integration of the published data, we attempt to assess the level of metal concentrations in igneous rocks formed in different geodynamic settings. Recently available rather sensitive methods of chemical analysis of fluid inclusions in minerals (LA-ICPMS etc.) make it possible to assess the concentrations of ore components in natural fluids and to compare them with concentrations in magmatic melts.

ORE ELEMENT CONTENTS IN NATURAL MELTS AND FLUIDS

Table 1 presents the information on number of publications reporting analytical results on 24 ore elements in magmatic silicate melts and natural fluids obtained in various periods of time. Note that 54% of the data on ore elements in magmatic melts and 77% of the data on the same elements in natural fluids have been published over the last 10 years (2005–2014).

Table 2 contains information on the number of publications and determinations of each ore element in magmatic silicate melts and fluids. For silicate melts, the representativeness of the data is shown for the main geodynamic settings: I, oceanic ridges; II, oceanic islands; III, island arcs; IV, active continental margins; V, intracontinental rifts and hotspots; VI, backarc basins, and the total for all terrestrial settings. We cannot list all 608 publications; therefore, in the notes to Table 2 we give references only to those works with 30 or more analyses of ore elements contained in melt inclusions or quenched glasses of volcanic rocks.

As been shown in our previous publications (Naumov et al., 2004, 2010, 2014; Kovalenko et a., 2006), the geometric mean is more adequate than the arithmetic mean for calculating rare element concentrations because of their lognormal distribution. This type of distribution for certain ore elements is exemplified in magmatic melts (Fig. 1) and in natural fluids (Fig. 2). The geometric mean was calculated under the condition that the value of induvidual determination does not deviate from the average value by more than 2σ with a probability of 95%. In addition, the possible occurrence of peaks in the considered total set of data is verified. Values with a probability of deviating from the average by more than 5% have been rejected, and afterward, the average was again recalculated. The mean element concentrations in melts inherent to certain geodynamic settings and to natural fluids are given in Table 3. In addition, the confidence intervals for each element are also given (first numeral, plus to the average and the second numeral, minus from the average).

The histograms of the SiO_2 distribution in natural magmatic melts typical of the main geodynamic settings are deduced from the compositions of homogeneous melt inclusions in minerals and quenched glasses of rocks (Fig. 3). The bimodal distribution is distinctly expressed for island arcs (III), active continental margins (IV), and intracontinental rifts and hotspots (V). Therefore, the mean contents of ore elements and confidence intervals are calculated for two SiO_2 contents: 40–62 wt % and >62 wt %. The data obtained presented in Table 4.

DISCUSSION

Analysis of the mean compositions of melts pertaining to a massif of data, which comprises various complexes with special history and formation conditions, makes it possible to consider the general geochemical tendencies (Kovalenko et al., 2007; Naumov et al., 2010). Figure 4 shows variations in the mean

Table 2. Representativeness of data on concentrations of ore elements in magmatic silicate melts ($SiO_2 \geqslant 40$ wt %) and natural fluids as deduced from compositions of melt inclusions in minerals and quenched glasses of volcanic rocks

Element	Number of publications and determinations							
	Magmatic silicate melts							Natural fluids
	I*	II	III	IV	V	VI	Σ**	
V	37 (1987)	51 (1686)	55 (1073)	18 (385)	63 (927)	12 (245)	235 (6328)	12 (93)
Cr	56 (2445)	66 (2137)	72 (1398)	22 (384)	89 (895)	15 (497)	315 (7787)	15 (77)
Co	25 (1154)	18 (394)	24 (393)	6 (48)	26 (242)	7 (133)	104 (2370)	30 (264)
Ni	34 (1443)	40 (1451)	30 (755)	9 (101)	44 (515)	11 (232)	169 (4507)	27 (232)
Cu	30 (1582)	21 (590)	36 (1081)	21 (679)	32 (422)	11 (308)	140 (4678)	123 (2866)
Zn	26 (1355)	21 (790)	33 (880)	14 (640)	31 (426)	7 (174)	123 (4275)	111 (2753)
Ga	20 (1540)	11 (362)	14 (372)	6 (188)	13 (163)	4 (66)	65 (2696)	17 (164)
Ge	3 (518)	1 (16)	1 (2)	–	2 (7)	2 (32)	8 (579)	17 (157)
As	3 (366)	5 (176)	11 (580)	10 (443)	9 (157)	4 (109)	38 (1835)	85 (2512)
Nb	59 (2730)	73 (3022)	106 (3355)	51 (1409)	147 (2825)	19 (523)	447 (13968)	20 (247)
Mo	6 (681)	9 (260)	15 (664)	11 (437)	19 (628)	5 (142)	58 (2812)	54 (880)
Ag	3 (573)	2 (28)	5 (263)	4 (75)	4 (66)	3 (63)	16 (1068)	66 (1125)
Cd	3 (644)	6 (167)	3 (6)	–	–	3 (63)	12 (880)	21 (95)
In	3 (643)	3 (128)	1 (2)	–	–	3 (63)	7 (836)	5 (35)
Sn	4 (652)	7 (334)	6 (56)	15 (477)	24 (509)	3 (63)	54 (2091)	37 (348)
Sb	3 (281)	7 (193)	8 (185)	7 (381)	6 (90)	3 (59)	30 (1192)	51 (1184)
Ta	41 (1939)	41 (1701)	53 (1627)	27 (587)	74 (1072)	11 (280)	240 (7233)	9 (91)
W	5 (721)	6 (164)	12 (403)	6 (253)	17 (357)	4 (74)	40 (1978)	36 (676)
Au	3 (191)	1 (3)	3 (127)	1 (35)	2 (22)	3 (89)	11 (467)	41 (756)
Tl	5 (598)	6 (181)	3 (117)	2 (157)	–	3 (53)	15 (1109)	15 (289)
Pb	35 (1794)	42 (1887)	72 (2271)	25 (955)	64 (1604)	15 (401)	244 (8929)	116 (3306)
Bi	4 (620)	5 (158)	5 (111)	4 (238)	6 (142)	3 (57)	24 (1331)	34 (389)
Th	53 (2275)	53 (1569)	89 (2748)	43 (1159)	127 (2475)	16 (422)	365 (10684)	25 (274)
U	47 (2176)	47 (2107)	79 (2455)	41 (1039)	104 (2088)	13 (354)	315 (10251)	35 (460)

* Here and in Table 3: main geodynamic settings (I, oceanic ridges; II, oceanic islands; III, island arcs; IV, active continental margins; V, continental rifts and hotspots; VI, backarc basins); ** all terrestrial settings. Number of determinations is given in parentheses. **Main publications on magmatic melts, period 1990–1999:** Devey et al., 1990; Hawkins et al., 1990; Webster and Duffield, 1994; Niu et al., 1996; Webster et al., 1996; Niu and Batiza, 1997; Wallace et al., 1999; period **2000–2009:** Anderson et al., 2000; Castillo et al., 2000; Danyushevsky et al., 2000; Sushchevskaya et al. (a), 2000; Sushchevskaya et al. (b), 2000; Slater et al.,2001; Sun et al., 2003; Halter et al., 2004; Perugini and Poli, 2004; Student and Bodnar, 2004; Sun et al., 2004; Workman et al., 2004; Simonov et al., 2005; Ren et al., 2005; Audetat and Pettke, 2006; Gurenko and Sobolev, 2006; Hammer et al., 2006; Liu et al., 2006; Mustard et al., 2006; Rickers et al., 2006; Beaudoin et al., 2007; Jordan et al., 2007; Sun et al., 2007; Zajacz and Halter, 2007; Sadofsky et al., 2008; Silant'ev et al., 2008; MacLennan, 2008; Sun et al., 2008; Arevalo et al., 2009; Collins et al., 2009; Rowe et al., 2009; Sisson et al., 2009; **period 2010–2014:** Audetat, 2010; Bouvier et al., 2010; Goss et al., 2010; Jenner et al., 2010; Ruscitto et al., 2010; Nikogosian and Bergen, 2010; Saunders et al., 2010; Audetat et al., 2011; Cottrell and Kelley, 2011; Frey et al., 2011; Gray et al., 2011; Holwell et al., 2011; Konig et al., 2011; McPhie et al., 2011; Sobolev et al., 2011; Waters et al., 2011; Wehrmann et al., 2011; Caulfield et al., 2012; Field et al., 2012; Guzmics et al., 2012; Jenner and O'Neill, 2012; Jenner et al., 2012; Kamenetsky and Eggins, 2012; Laubier et al., 2012; Neave et al., 2012; Pritchard and Larson, 2012; Salisbury et al., 2012; Timm et al., 2012; Berlo et al., 2013; Johnson et al., 2013; Lerchbaumer and Audetat, 2013; Nadeau et al., 2013; Robertson et al., 2013; Vlastelic et al., 2013; Metrich et al., 2014. **Main publications on natural fluids, period 1996–2009:** Rosenbaum et al., 1996; Ulrich et al., 2001; Vanko et al., 2001; Audetat and Pettke, 2003; Zaw et al., 2003; Beuchat et al., 2004; Rusk et al., 2004; Stoffell et al., 2004; Thebaud et al., 2006; Baker et al., 2006; Wallier et al., 2006; Klemm et al., 2007; Zedgenizov et al., 2007; Audetat et al., 2008; Baker et al., 2008; Stoffell et al., 2008; Luders et al., 2009; Pudack et al., 2009; Su et al., 2009; Wilkinson et al., 2009; **period 2010–2014:** Bortnikov et al., 2010; Kurosawa *et al.*, 2010; Kouzmanov et al., 2010; Allan et al., 2011; Hanley et al., 2011; Kotzeva et al., 2011; LeFort et al., 2011; Leisen et al., 2012; Li et al., 2012; Pettke et al., 2012; Richard et al., 2012; Seo et al., 2012; Hammerli et al., 2013; Lerchbaumer and Audetat, 2013; Marsala et al., 2013; Miron et al., 2013; Silva et al., 2013; Sirbescu et al., 2013; Fusswinkel et al., 2014; Hurtic et al., 2014.

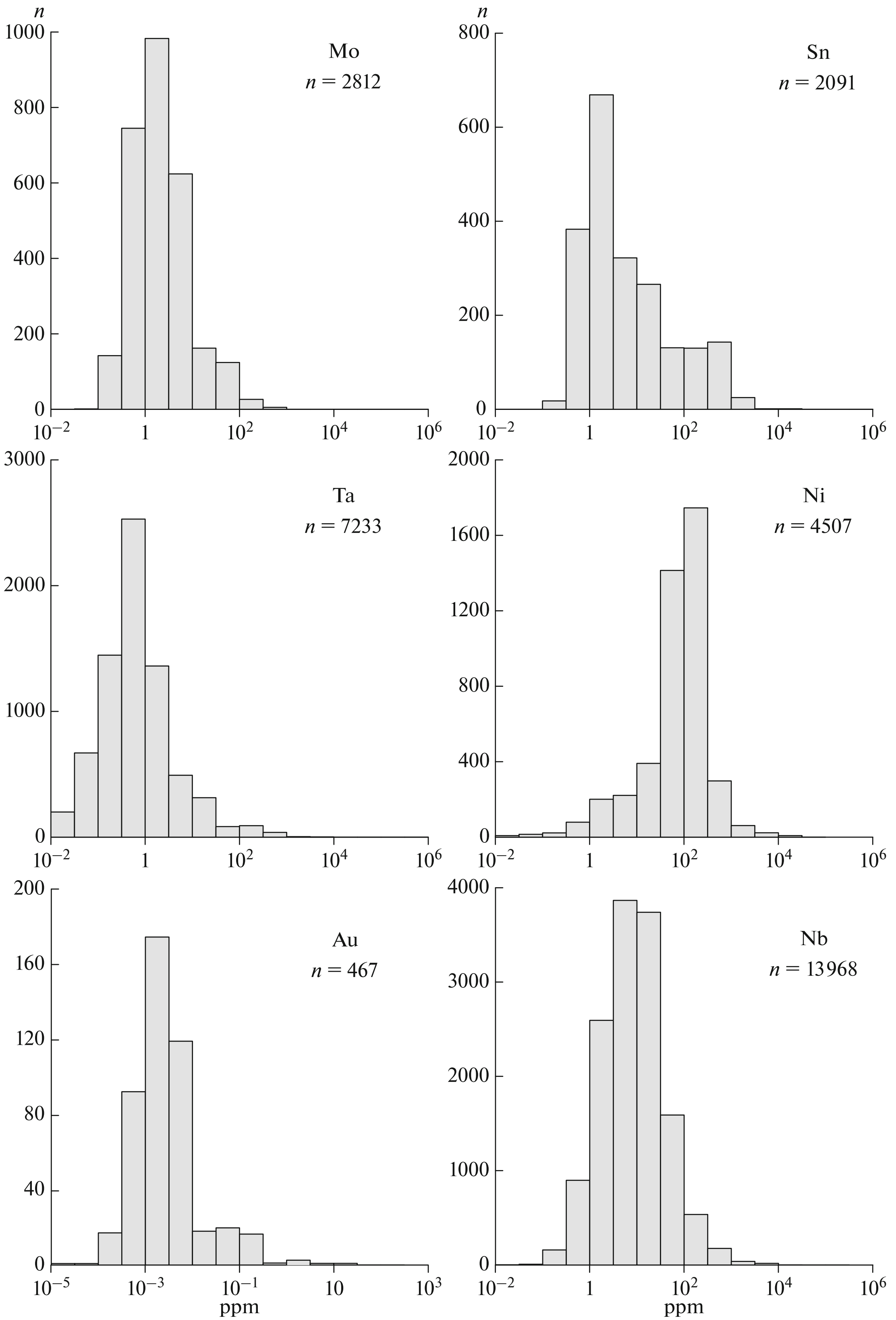

Fig. 1. Histograms of Mo, Sn, Ta, Ni, Au, and Nb distribution in magmatic melts; *n* is number of determinations.

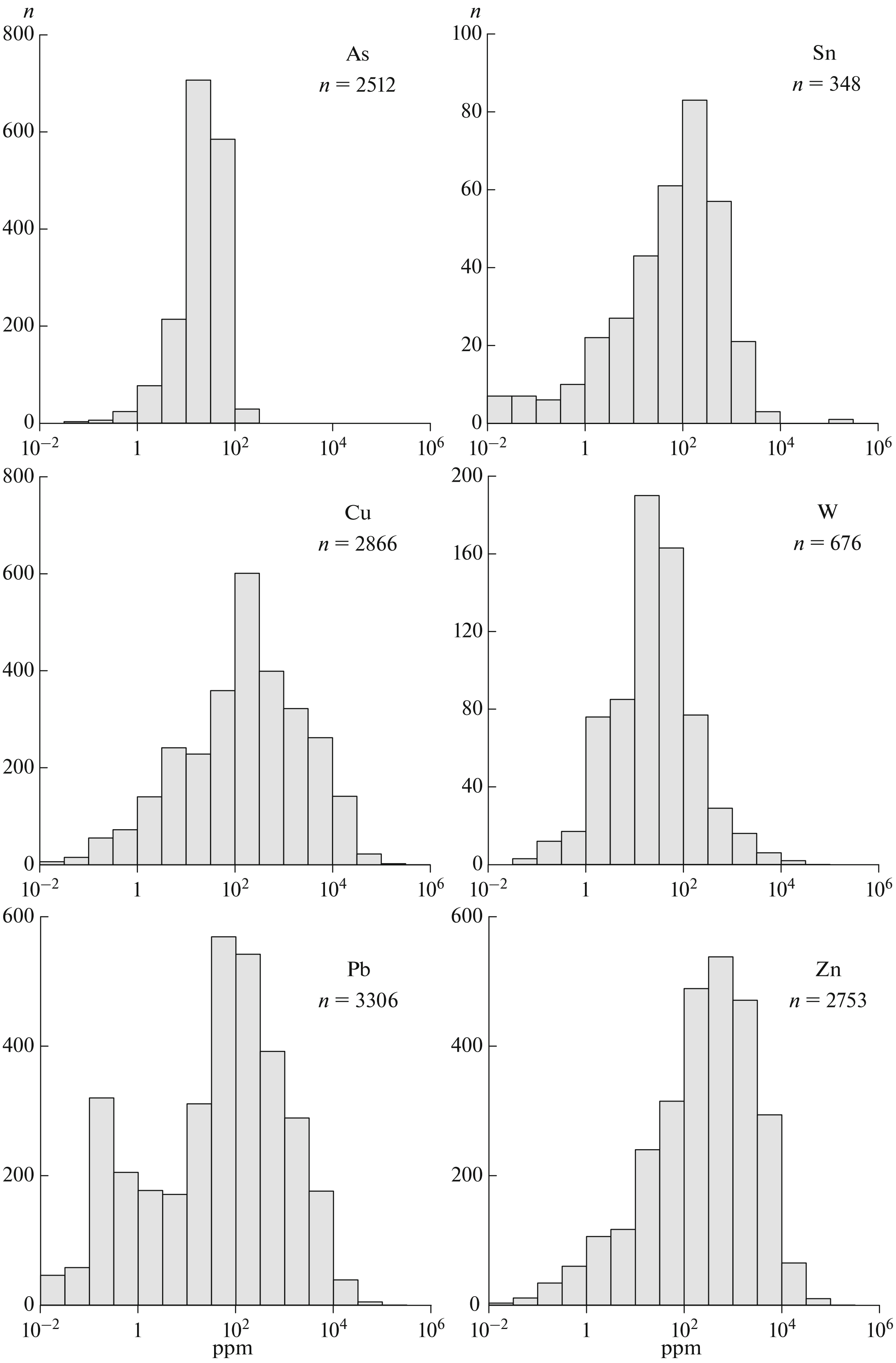

Fig. 2. Histograms of As, Sn, Cu, W, Pb, and Zn distribution in natural fluids; *n* is number of determinations.

Table 3. Concentrations of ore elements in magmatic silicate melts (SiO_2 > 40 wt %) and natural fluids as deduced from compositions of melt inclusions in minerals and quenched glasses of volcanic rocks in various geodynamic settings (I–VI)

Element	Magmatic melts							Natural fluids
	I	II	III	IV	V	VI	Σ	
V, ppm	273	286	145	221	8.95	284	256	1.36
	+95/–70	+99/–74	+936/–126	+161/–93	+136/–8.40	+114/–82	+259/–129	+24.4/–1.29
Cr, ppm	309	323	54.2	48.3	247	296	266	19.5
	+242/–136	+472/–192	+557/–49.4	+339/–42.3	+2932/–228	+1020/–229	+710/–194	+587/–18.9
Co, ppm	44.0	44.8	12.1	24.9	4.22	42.7	39.0	2.07
	+6.5/–5.7	+17.2/–12.4	+54.5/–9.9	+80.0/–19.0	+26.48/–3.64	+27.3/–16.6	+29.5/–16.8	+35.4/–1.96
Ni, ppm	102	126	8.2	32.6	45.3	73.9	88.5	15.0
	+61/–38	+154/–69	+39.5/–6.8	+89.9/–23.9	+1025/–43.4	+157/–50.2	+212/–62.5	+189/–13.8
Cu, ppm	75.2	94.7	38.4	40.3	19.3	79.0	66.4	144
	+21.6/–16.8	+63.1/–37.9	+200/–32.2	+185/–33.1	+343/–18.2	+167.1/–53.6	+130/–44.0	+1997/–134
Zn, ppm	84.1	128	56.8	48.7	72.5	83.1	77.6	298
	+43.5/–28.7	+89/–52	+60.2/–29.2	+46.2/–23.7	+121/–45.3	+42.3/–28.0	+81.5/–39.8	+3115/–272
Ga, ppm	17.8	29.1	16.0	18.4	24.1	17.2	17.9	1.56
	+2.6/–2.3	+13.4/–9.2	+3.6/–2.9	+3.8/3.2	+19.5/–10.8	+2.1/–1.8	+4.0/–3.2	+20.27/–1.45
Ge, ppm	1.51	1.56	–	–	2.36	1.77	1.53	4.68
	+0.12/–0.11	+0.07/–0.06	–	–	+1.01/–0.71	+0.12/–0.11	+0.16/–0.14	+33.74/–4.11
As, ppm	0.20	1.00	2.66	156	16.6	1.19	2.15	47.3
	+0.22/–0.10	+1.42/–0.59	+3.00/–1.41	+3687/–149	+44.0/–12.1	+3.10/–0.86	+13.05/–1.85	+203/–38.4
Nb, ppm	2.86	12.8	3.15	8.34	40.5	1.35	6.76	2.25
	+5.01/–1.82	+16.3/–7.2	+6.29/–2.10	+12.07/–4.93	+102.3/–29.0	+2.20/–0.84	+22.21/–5.18	+15.34/–1.96
Mo, ppm	0.63	4.88	1.30	6.70	4.06	0.51	1.46	16.1
	+0.35/–0.23	+3.82/–2.14	+0.82/–0.50	+44.89/–5.83	+4.57/–2.15	+0.66/–0.29	+3.02/–0.98	+80.8/–13.4
Ag, ppb	21.2	24.4	32.4	152	182	34.2	26.7	2354
	+7.5/–5.5	+26.8/–12.8	+31.3/–15.9	+1382/–137	+391/–124	+14.4/–10.2	+28.8/–13.4	+13100/–1995
Cd, ppb	139.4	134.5	–	–	–	142.8	139.5	2739
	+28.7/–23.8	+28.6/–23.6	–	–	–	+25.1/–21.4	+38.3/–30.0	+31920/–2520
In, ppb	77.6	89.4	–	–	–	70.7	79.1	1080
	+18.2/–14.7	+6.3/–5.9	–	–	–	+15.2/–12.5	+18.3/–14.8	+7520/–950
Sn, ppm	1.02	4.74	0.98	38.06	14.47	0.83	3.14	45.1
	+0.41/–0.29	+10.29/–3.24	+1.18/–0.53	+1097/–36.78	+31.93/–9.96	+0.28/–0.21	+15.43/–2.61	+356/–40.0
Sb, ppm	0.013	0.10	0.11	31.28	0.73	0.03	0.19	8.00
	+0.009/–0.005	+0.28/–0.07	+0.17/–0.07	+1156/–30.46	+1.79/–0.52	+0.06/–0.02	+2.22/–0.17	+35.0/–6.51
Ta, ppm	0.29	0.91	0.45	0.79	3.84	0.08(246)	0.65	0.19
	+0.43/–0.17	+0.76/–0.42	+1.03/–0.31	+3.23/–0.63	+11.11/–2.86	+0.15/–0.05	+1.74/–0.47	+1.44/–0.17
W, ppm	0.03	0.29	0.46	58.0	5.25	0.07	0.46	19.1
	+0.08/–0.02	+ 0.17/–0.11	+0.94/–0.31	+103.2/–37.1	+10.04/–3.45	+0.09/–0.04	+4.50/–0.42	+88.8/–15.7
Au, ppb	1.09	–	2.76	57.3	74.0	2.34	1.77	557
	+1.11/–0.55	–	+3.36/–1.52	+152/–41.6	+172/–51.8	+3.52/–1.40	+3.35/–1.16	+3996/–489
Tl, ppb	9.87	59.0	63.2	634	–	60.1	20.5	2834
	+8.15/–4.46	+100.0/–37.1	+88.6/–36.9	+307/–207	–	+225/–47.4	+76.4/–16.2	+4233/–1697
Pb, ppm	0.64	1.01	9.98	10.74	27.14	1.15	2.33	17.6
	+0.40/–0.25	+1.15/–0.54	+23.64/–7.02	+20.58/–7.06	+39.86/–16.15	+1.82/–0.70	8.76/–1.84	+297/–16.7
Bi, ppm	0.007	0.017	0.033	8.88	1.15	0.019	0.059	3.14
	+0.002/–0.002	+0.010/–0.006	0.046/–0.019	+26.86/–6.67	+1.55/–0.66	+0.020/–0.010	+0.66/–0.05	+12.48/–2.51
Th, ppm	0.36	1.37	1.87	3.47	15.13	0.66	2.33	1.01
	+0.68/–0.23	+3.02/–0.94	+8.60/–1.54	+11.32/–2.66	+25.91/–9.55	+1.15/–0.41	+14.08/–2.00	+10.65/–0.92
U, ppm	0.09	0.52	1.21	1.46	5.07	0.34	0.92	1.50
	+0.15/–0.06	+0.80/–0.31	+3.38/–0.89	+2.97/–0.98	+8.10/–3.12	+0.77/–0.23	+5.71/–0.79	+21.78/–1.40

The element contents were calculated as the geometric mean under the condition that the value of an individual determination does not deviate from the average value by more than 2σ with a probability of 95%; the deviation is given under the mean content: the left numeral is plus to the mean, and the right numeral is minus from the mean).

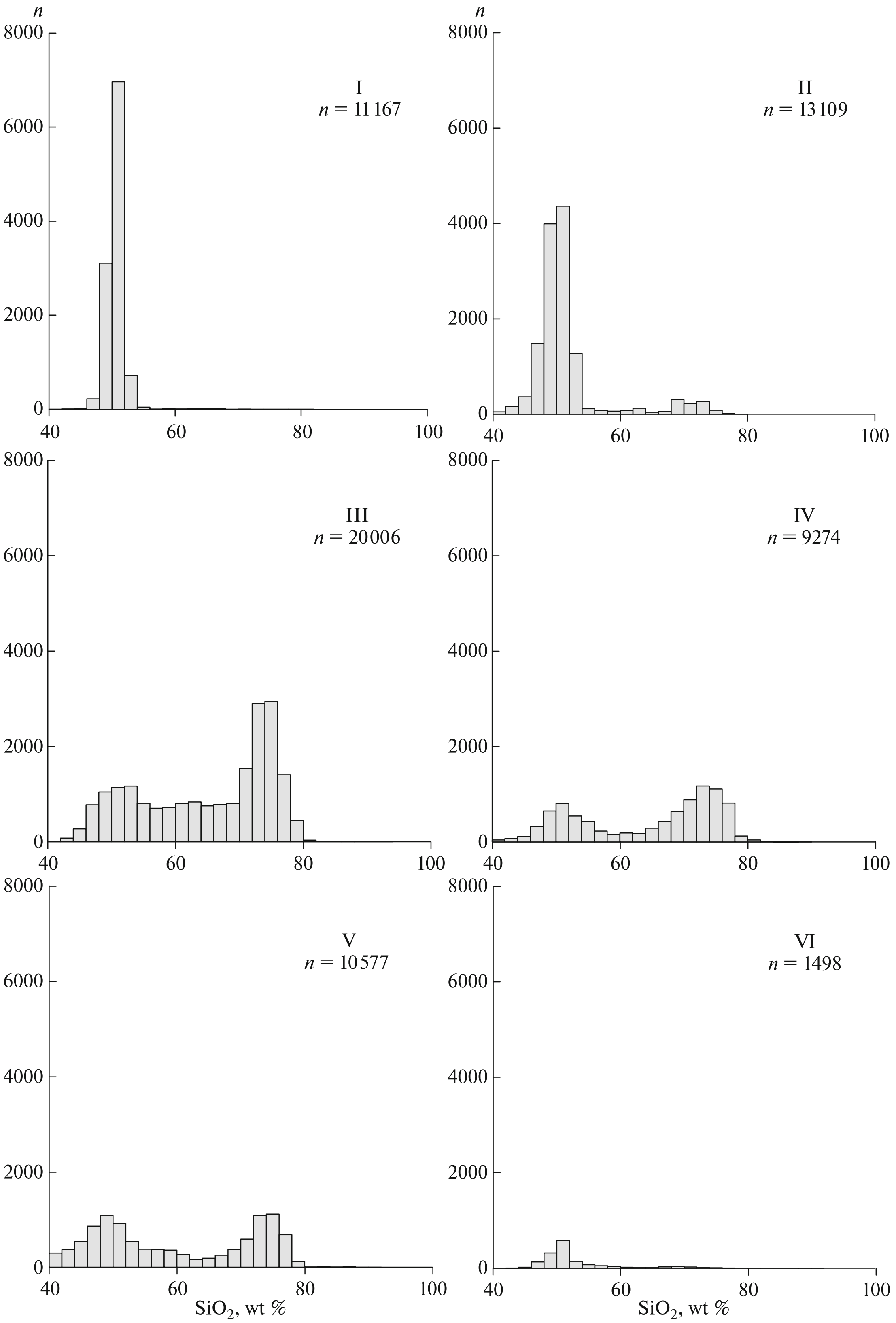

Fig 3. Histograms of SiO_2 distribution in magmatic melts from main geodynamic settings (I–VI) as deduced from composition of homogeneous melt inclusions in minerals and of quenched glasses of rocks; *n* is number of determinations. I, mid-ocean ridges; II, oceanic islands; III, island arcs; IV, active continental margins; V, intracontinental rifts and hotspots; VI, back arc basins.

Table 4. Concentrations of ore elements in magmatic silicate melts ($SiO_2 \geqslant 40$ wt %) from island arcs (III), active continental margins (IV), continental rifts and hotspots (V) as deduced from compositions of melt inclusions in minerals and quenched glasses of volcanic rocks

Element	III		IV		V	
	SiO_2 = 40–62 wt %	SiO_2 > 62 wt %	SiO_2 = 40–62 wt %	SiO_2 > 62 wt %	SiO_2 = 40–62 wt %	SiO_2 > 62 wt %
V, ppm	317 (642)	8.0 (431)	231 (337)	5.9 (48)	229 (378)	2.4 (549)
	+141/–98	+31.6/–6.4	+77/–58	+29.6/–4.9	+312/–132	+4.6/–1.6
Cr, ppm	116 (1035)	4.3 (363)	101 (274)	4.4 (110)	488 (679)	3.8 (216)
	+672/–99	+13.8/–3.3	+312/–76	+13.0/–3.3	+1856/–386	+9.8/–2.7
Co, ppm	31.9 (200)	2.8 (193)	33.4 (36)	1.4 (12)	19.7 (140)	1.2 (102)
	+10.1/–7.7	+10.5/–2.2	+70.4/–22.6	+1.3/–0.7	+83.2/–15.9	+6.1/–1.0
Ni, ppm	20.5 (509)	1.9 (246)	38.3 (86)	10.4 (15)	288 (385)	0.89 (130)
	+59.9/–15.3	+3.5/–1.2	+103.5/–28.0	+18.4/–6.7	+853/–215	+8.13/–0.80
Cu, ppm	119 (338)	10.2 (743)	162 (188)	22.1 (491)	196 (167)	4.49 (255)
	+91/–52	+79.6/–9.1	+384/–114	+54.8/–15.8	+712/–154	+29.30/–3.89
Zn, ppm	84.3 (302)	44.6 (578)	92.2 (93)	45.4 (547)	118 (131)	56.9 (295)
	+30.3/–22.3	+43.8/–22.1	+120.5/–52.2	+35.0/–19.8	+108/–50	+116.1/–38.2
Ga, ppm	16.6 (195)	15.0 (177)	26.2 (23)	18.0 (165)	23.2 (72)	25.5 (91)
	+ 2.4/–2.1	+5.0/–3.7	+9.4/–6.9	+2.9/–2.5	+17.1/–9.8	+25.9/–12.9
As, ppm	1.31 (265)	4.32 (315)	868 (19)	141 (424)	3.4 (8)	17.4 (149)
	+2.21/–0.82	+2.79/–1.70	+970/–458	+3360/–136	+1.6/–1.1	+44.4/–12.5
Nb, ppm	1.25 (1475)	7.11 (1880)	6.11 (722)	9.65 (687)	26.76 (891)	45.57 (1934)
	+1.80/–0.74	+3.94/–2.53	+13.53/–4.21	+9.30/–4.74	+91.76/–20.72	+102.07/–31.51
Mo, ppm	0.60 (123)	1.48 (541)	11.8 (22)	6.8 (415)	2.0 (17)	4.1 (611)
	+6.57/–0.29	+0.76/–0.50	+17.4/–7.0	+48.4/–6.0	+2.4/–1.1	+4.6/–2.2
Ag, ppb	27.6 (92)	39.2 (171)	3.79 (10)	90.3 (65)	–	182 (66)
	+15.3/–9.8	+40.8/–20.0	+11.2/–2.8	+460.2/–75.5		+391/–124
Sn, ppm	0.72 (28)	1.36 (28)	791 (23)	31.4 (454)	15.6 (15)	14.5 (494)
	+0.36/–0.24	+1.11/–0.61	+889/–418	+881/–30.3	+87.5/–13.3	+31.6/–9.9
Sb, ppm	0.07 (128)	0.56 (57)	34.0 (18)	31.2 (363)	1.4 (7)	0.65 (83)
	+0.06/– 0.03	+1.25/–0.39	+12.4/–9.1	+1260/–30.4	+2.9/–1.0	+1.45/–0.45
Ta, ppm	0.09 (631)	0.73 (996)	0.49 (301)	8.39 (286)	1.60 (389)	7.41 (683)
	+0.18/–0.06	+0.52/–0.30	+0.76/–0.30	+183/–8.02	+3.84/–1.13	+17.80/–5.23
W, ppm	0.17 (248)	0.99 (155)	52.1 (16)	56.8 (237)	1.18 (16)	5.79 (341)
	+0.30/–0.11	+2.34/–0.70	+159.6/–39.3	+101.7/–36.5	+1.65/–0.69	+10.99/–3.79
Au, ppb	2.39 (101)	3.68 (26)	–	57.3 (35)	94.0 (8)	58.2 (14)
	+2.81/–1.29	+3.97/–1.91		+152.2/–41.6	+240.1/–67.6	+111.6/–38.2
Tl, ppb	53.4 (91)	266 (26)	82.0 (22)	646 (135)	–	–
	+41,4/–23.3	+558/–180	+33.3/–23.7	+196/–150		
Pb, ppm	2.59 (930)	18.33 (1341)	4.51 (490)	19.59 (465)	3.51 (385)	33.4 (1219)
	+3.47/–1.49	+13.62/–7.81	+5.68/–2.51	+8.19/–5.77	+9.11/–2.53	+24.6/–14.2
Bi, ppm	0.024 (80)	0.41 (31)	17.51 (13)	8.24 (225)	–	1.15 (138)
	+0.011/–0.008	+1.77/–0.33	+10.73/–6.65	+27.53/–6.34		+1.55/–0.66
Th, ppm	0.62 (1278)	10.8 (1470)	1.10 (507)	11.85 (652)	2.30 (680)	21.73 (1795)
	+0.87/–0.36	+11.0/–5.5	+1.32/–0.60	+12.48/–6.08	+7.57/–1.76	+20.33/–10.51
U, ppm	0.37 (1074)	2.19 (1381)	0.67 (410)	3.30 (629)	1.34 (559)	8.58 (1529)
	+0.52/– 0.21	+1.60/–0.92	+0.89/–0.38	+3.06/–1.59	+4.55/–1.04	+7.63/–4.04

Numbers of determinations are shown in parentheses.

glasss compositions normalized to the primitive mantle (Palme and O'Neill, 2003) versus the partition coefficients between olivine and the basic melt estimated from the experimental data. Normalization to the composition of the primitive mantle is widely used in geochemical studies and is informal in our case. In currently discussed geodynamic models, the global crustal reservoir is regarded as a product of magmatic fractionation of the primitive mantle, and this makes the ratio of the element contents in the mantle and crust an important geochemical indicator (Palme and O'Neill, 2003). The partition coefficient between olivine and the melt ($D^{\text{Ol-Melt}}$) also serves as an important integral parameter. Olivine is the major mantle phase and one of leading minerals participating in fractionation of basic magmas under crustal conditions. In addition, the distribution of elements between olivine and the melt is similar in many aspects to those of other major silicate minerals in mafic systems (pyroxene, garnet, feldspar). Therefore, the $D^{\text{Ol-Melt}}$ value can be regarded as a generalized characteristic of the degree of incompatibility of an element in mafic magmatic systems. The advantage of olivine as compared, for example, to pyroxene is the simple chemical composition of this mineral and thus the lower variability of $D^{\text{Ol-Melt}}$ for a specific element. Meanwhile, the interval of partition coefficients for olivine is wider than for other minerals, and this is also convenient for considering chemical element behavior.

The established trends can so far be assessed as semiquantitative. The data on contents of a certain ore elements in natural melts are limited, and the determinaton of low contents may be not sufficiently exact. In addition, the experimental data for many of the considered elements are also very limited. In particular, for such elements as As, Ag, Cd, In, Sn, Tl, and Bi, determinations are available only from two runs at 10 and 20 kbar (Adam and Green, 2006). Nevertheless, the difference in geodynamic settings is rather distinctly fixed in Fig. 4.

In general, the increase in the normalized mean contents correlates with a decrease in the $D^{\text{Ol-Melt}}$ for all settings. This correlation indicates the important role of mineral–melt equilibria in the balance of ore elements. The lowest degree of element fractionation is established for setting I (mid-ocean ridges) and VI (backarc basins). They are characterized by growth in the mean values with a decrease in $D^{\text{Ol-Melt}}$ from Ni ($D^{\text{Ol-Melt}} \sim 10$) to Cu ($D^{\text{Ol-Melt}} \sim 0.1$). Approximately constant and moderate normalized concentrations are observed for all more- incompatible elements. No appreciable difference in the behavior of fluid-mobile and other components has been established. This pattern fits the scheme of melt formation in the course of depleted mantle melting at comparatively low contents of strongly incompatible elements and differentiation of melts for a low fugacity of volatile components. Tungsten occupies a special place and is characterized by depletion with respect to the primitive mantle (like for strongly compatible Cr and Co) for a very low $D^{\text{Ol-Melt}}$. The reason for this is not clear. The compatibility of tungsten during melting and crystallization would require retention of a phase selectively concentrating W. Taking into account that low W contents are a persistent feature traced in other settings (see below), such a suggestion seems a little unlikely. It cannot be ruled out that the W content in the primitive mantle model is overestimated by Palme and O'Neill (2003), so that the concentration of this element in real mantle material is actually much lower. Systematic analytical errors when studying glassy inclusions are also possible.

In melts of oceanic islands (setting II), the increase in the mean contents with a decrease in $D^{\text{Ol-Melt}}$ proceeds up to maximum incompatible elements. This is consistent with the idea of a fertile magma source beneath oceanic islands as compared to the depleted mantle. Like melts in settings I and VI, W appreciably deviates from the general trend toward low contents and Mo toward high contents. In addition, strong enrichment in some fluid-mobile elements (Sb, Sn, Tl, In) is traced. This tendency becomes especially perceptible in melts of island arcs (III) and active continental margins (IV). Enrichment of melts pertaining to setting IV with respect to Au, Sb, Tl, Bi, As, and Sn is especially significant. These elements do not reveal a general trend to increase in normalized contents with a decrease in $D^{\text{Ol-Melt}}$. It is evident that crystallization of mafic magmas is not a crucial controlling process, and transfer with the fluid phase can play a more significant role. Similar Mo and W behavior is typical of this setting. This change in behavior of this pair of elements is evidence that the aforementioned deviations in settings I and II can hardly be a result of analytical errors.

For the melts of continental magmatism (setting V), a linear trend for moderately and highly compatible elements is combined with approximately similar enrichment in all elements, for which $D^{\text{Ol-Melt}} < 0.005$, as well as for Au and Sb.

The probable effect of fluid mass transfer is illustrated by the relationship of the mean normalized element contents depending on the average contents in fluid inclusions (Fig. 5). The data for settings I and IV are the most indicative (Fig. 5). These plots may be described only in qualitative terms, because the effect of fluids is always combined with those of melting and crystallization; the contents of elements in solutions and melts are also linked by a significant positive correlation. In the given plots, it is important that the lack of a correlation between the indicated parameters for setting I is combined with the significant correlation for setting IV. This can be regarded as evidence for the appreciable role of fluid transfer of incompatible elements in settings related to subduction and collision.

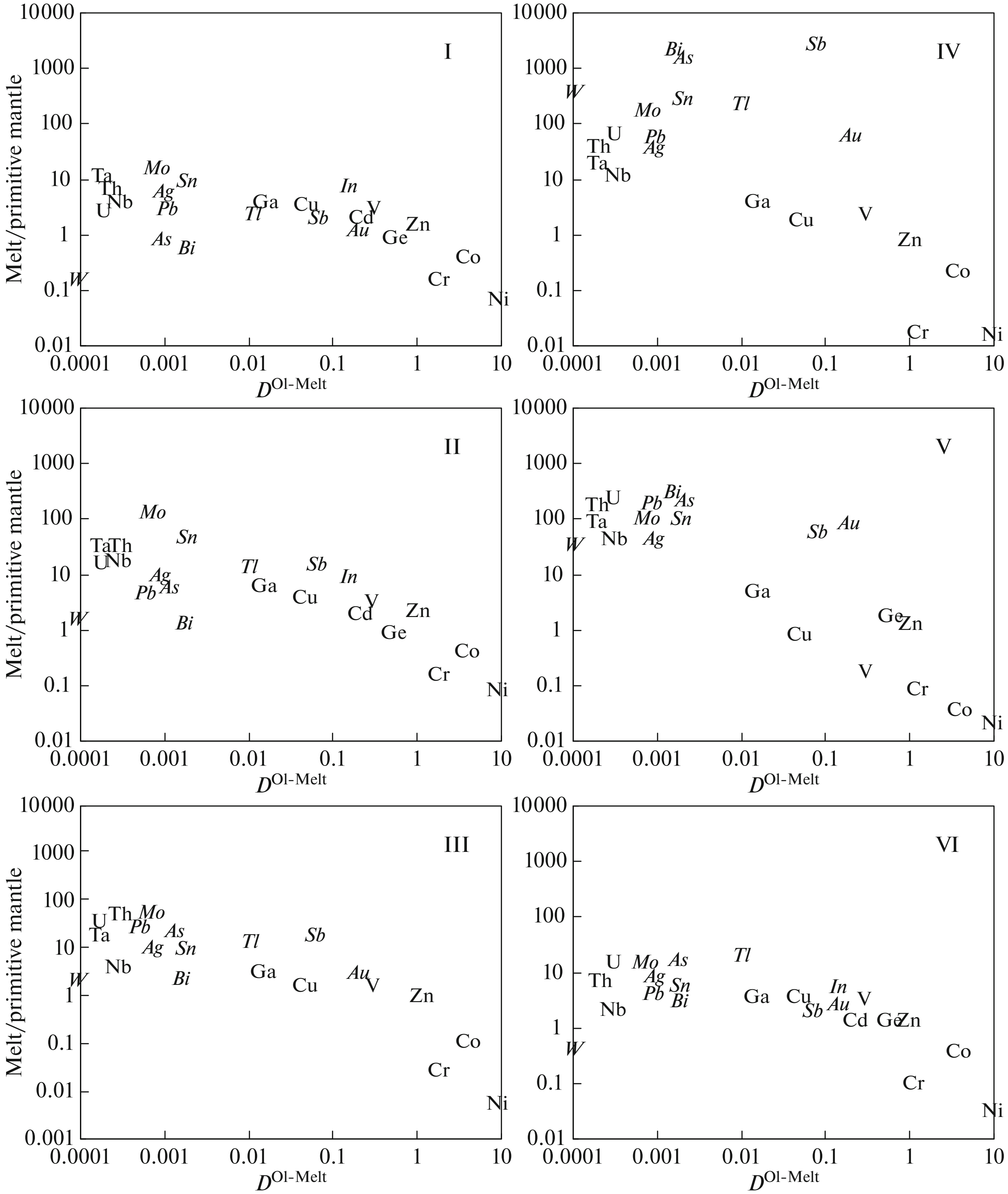

Fig. 4. Mean compositions of melts from various geodynamic settings normalized to primitive mantle (Palme and O'Neill, 2003) versus mean partition coefficients of elements between olivine and basic melt ($D^{\text{Ol-Melt}}$). Partition coefficient values are an average of published experimental data for pressure <50 kbar and melts containing 45–55 wt % SiO_2 compiled in MELT database (Girnis, 2003). Fluid-mobile elements characterized by high contents in fluid inclusions (> 100 by normalizing to primitive mantle) are marked in italic type.

As mentioned above, island arcs (III), active continental margins (IV), intracontinental rifts and areas of hotspots (V) are characterized by a bimodal type of SiO_2 distribution. Therefore, the mean contents of ore elements and their consistent intervals for these settings have been calculated for two intervals of SiO_2 contents: 40–62 wt % and higher than 62 wt %. As follows from the presented data (Table 4), the concentrations of V, Cr, Co, Ni, Cu, Zn in felsic melts are much lower than in basic melts. Inverse concentration pro-

Table 5. Comparison of ore element concentrations and volatile components in basic magmatic silicate melts from mid-ocean ridges (I) and active continental margins (IV) as deduced from compositions of melt inclusions in minerals and quenched glasses of volcanic rocks

Element	I	IV
	Solid	
V, ppm	273 (1987)	231 (337)
Cr, ppm	309 (2445)	101 (274)
Co, ppm	44.0 (1154)	33.4 (36)
Ni, ppm	102 (1443)	38.3 (86)
Cu, ppm	75.2 (1582)	162 (188)
Zn, ppm	84.1 (1355)	92.2 (93)
Ga, ppm	17.8 (1540)	26.2 (23)
As, ppm	0.20 (366)	868 (19)
Nb, ppm	2.86 (2730)	6.11 (722)
Mo, ppm	0.63 (681)	11.8 (22)
Sn, ppm	1.02 (652)	791 (23)
Sb, ppm	0.013 (281)	34.0 (18)
Ta, ppm	0.29 (1939)	0.49 (301)
W, ppm	0.03 (721)	52.1 (16)
Tl, ppb	9.87 (598)	82.0 (22)
Pb, ppm	0.64 (1794)	4.51 (490)
Bi, ppm	0.007 (620)	17.5 (13)
Th, ppm	0.36 (2275)	1.10 (507)
U, ppm	0.09 (2176)	0.67 (410)
	Volatile	
H_2O, wt %	0.25 (2007)	2.01 (1335)
Cl, ppm	90 (3129)	770 (2737)
S, ppm	1020 (3164)	900 (2492)

Numbers of determinations are shown in parentheses.

portions have been established for Nb, Ta, W, Pb, Th, and U.

The concentrations of ore elements and volatile components contained in basic silicate melts of mid-ocean ridges (I) and active continental magins (IV) are compared in Table 5. Only V, Cr, Co, and Ni concentrations in melts of mid-ocean ridges are higher than in melts of active continental margins. All other elements are characterized by inverse proportions. Melts of active continental margins are also enriched in water as compared to melts of oceanic islands (2.0 and 0.25 wt %, respectively) and in chlorine (770 and 90 ppm, respectively).

The links between (i) various ore deposits, (ii) igneous rocks with which they are associated, and (iii) geotectonic settings where they formed are of the constant interest primarily because the revelation of these links makes it possible to define important empirical criteria for forecasting and prospecting economic mineralization and to specify targets and territories of works.

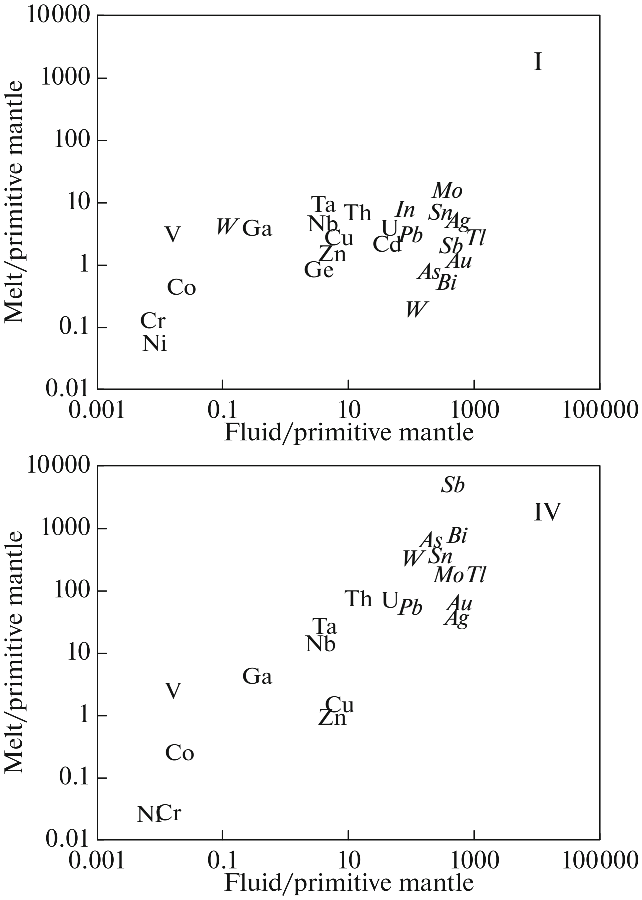

Fig. 5. Covariations of mean contents of ore elements in melts and fluids in settings I and IV. Plot shows appreciably increasing correlation by transition of settings related to melting of depleted mantle to settings where recycling of crustal material plays significant role.

One such criterion can be the degree of relative enrichment of magmatic melts in certain ore elements. In order to estimate such a degree for each of thegeodynamic settings considered in this paper, the concentration coefficients (Cc) have been calculated using the data collected in Table 3. We define Cc as theratio of the mean content of an element in a certain setting to the mean content of this element in all settings (Σ in Table 3). The Cc values are shown in Table 6. Ga, Ge, Cd, In, and Tl have been excluded from consideration, because they commonly do not make up large self-dependent accumulations in the Earth's crust and are commonly dispersed in minerals from ore deposits.

Three groups (associations) of chemical elements are distinguished by Cc values in Table 6. They are characterized by (1) slight relative enrichment of the magmatic melt (Cc = 1–2, light type); (2) substantial enrichment (Cc > 2, boldface), and (3) depletion (Cc < 1, italics). These associations reveal a similar

Table 6. Concentration coefficient (Cc) of ore elements in magmatic melts accommodated in main terrestrial geodynamic settings

Element	Geodynamic setting					
	I	II	III	IV	V	VI
V	1.1	1.1	*0.6*	*0.9*	*0.04*	1.1
Cr	1.2	1.2	*0.2*	*0.2*	*0.9*	1.1
Co	1.1	1.1	*0.3*	*0.6*	*0.1*	*0.1*
Ni	1.1	1.4	*0.1*	*0.4*	*0.5*	*0.8*
Cu	1.1	1.4	*0.6*	*0.6*	*0.3*	1.2
Zn	1.1	1.6	*0.7*	*0.6*	*0.9*	1.1
Pb	*0.3*	*0.4*	**4.3**	**4.6**	**12**	*0.5*
Bi	*0.1*	*0.3*	*0.6*	**150**	**19**	*0.3*
Au	*0.6*	–	1.6	**32**	**42**	1.3
Ag	*0.8*	*0.9*	1.2	**5.7**	**6.8**	1.3
Mo	*0.4*	**3.3**	*0.9*	**4.6**	**2.8**	*0.3*
W	*0.1*	*0.6*	1.0	**126**	**11**	*0.1*
Sn	*0.3*	1.5	*0.3*	**12**	**4.6**	*0.3*
Sb	*0.1*	*0.5*	*0.6*	**164**	**3.8**	*0.2*
As	*0.1*	*0.5*	1.2	**73**	**7.7**	*0.5*
Ta	*0.4*	1.4	*0.7*	1.2	**5.9**	*0.1*
Nb	*0.4*	1.9	*0.5*	1.2	**6.0**	*0.2*
Th	*0.02*	*0.6*	*0.8*	1.5	**6.5**	*0.3*
U	*0.1*	*0.6*	1.3	1.6	**5.5**	*0.4*

Slightly enriched values (Cc = 1–2) are in light type; substantially enriched values (Cc > 2) are boldfaced, and relatively depleted values (Cc < 1) are italicized.

behavior in various geodynamic settings and can be regarded as indicators of their potential productivity with respect to the given metals.

The first of these associations (V, Cr, Co, Ni, Cu, and Zn) is typical of magmatic melts occurring in setting I (oceanic ridges) and II (oceanic islands) with alkali basalts commonly related to mantle plumes and hotspots. A similar association, except for Co and Ni, has been also established for melts of backarc basins (setting VI, Table 6). In general, depletion in Pb, Bi, Au, Ag, Mo, W, Sn, Sb, As, Ta, Nb, Th, and U (Cc < 1) is inherent to magmas of these settings. Some exclusions, however, are also known: a slight enrichment of melts in Mo, Sn, Ta, and Nb has been established in setting II, and Au and Ag in setting VI.

Island-arc magmatic melts (setting III) are characterized by Pb, Au, As, and U, which generally correspond to the geochemical profiles of porphyry and epithermal families.

The most extensive and striking geochemical association is typical of magmatic melts at active continental margins (IV) and of intracontinental rifts (V). This association is represented by a group of elements (Pb, Bi, Au, Ag, Mo, W, Sn, Sb, As, Ta, Nb, Th, and U), which are characteristic of nonferrous, noble, rare, and radioactive ores formed in the above settings. The almost complete identity of metal contents in magmatic melts at active continental margins and zones of intracontinental rifts (settings IV and V) is noteworthy. They differ only in higher Bi, Mo, W, Sn, Sb, and As concentrations in setting IV, and Pb, Au, Ag, Ta, Nb, Th, and U in setting V (Table 6).

ACKNOWLEDGMENTS

We thank V.Yu. Prokof'ev and B.N. Ryzhenko for their comments and discussion. This study was supported by the Russian Foundation for Basic Research (project nos. 13-05-00450, 16-05-00622).

REFERENCES

Adam, J. and Green, T., Trace element partitioning between mica- and amphibole-bearing garnet lherzolite and hydrous basanitic melt: 1. Experimental results and the investigation of controls on partitioning behaviour, *Contrib. Mineral. Petrol.,* 2006, vol. 152, pp. 1–17.

Allan, M.M., Morrison, G.W., and Yardley, B.W.D., Physicochemical evolution of a porphyry-breccia system: a laser ablation ICP-MS study of fluid inclusions in the Mount Leysbon Au Deposit, Queensland, Australia, *Econ. Geol.,* 2011, vol. 106, pp. 413–436.

Anderson, A.T., Davis, A.M., and Lu, F., Evolution of Bishop tuff rhyolitic magma based on melt and magnetite inclusions and zoned phenocrysts, *J. Petrol.,* 2000, vol. 41, pp. 449–473.

Arevalo, R., Jr., McDonough, W.F., and Luong, M., The K/U ratio of the silicate Earth: insights into mantle composition, structure and thermal evolution, *Earth Planet. Sci. Lett.,* 2009, vol. 278, pp. 361–369.

Audetat, A. and Pettke, T., The magmatic-hydrothermal evolution of two barren granites: a melt and fluid inclusion study of the Rito del Medio and Canada Pinabete plutons in northern New Mexico (USA), *Geochim. Cosmochim. Acta,* 2003, vol. 67, pp. 97–121.

Audetat, A. and Pettke, T., Evolution of a porphyry-Cu mineralized magma system at Santa Rita, New Mexico (USA), *J. Petrol.,* 2006, vol. 47, pp. 2021–2046.

Audetat, A., Pettke, T., Heinrich, C.A., and Bodnar, R.J., The composition of magmatic-hydrothermal fluids in barren and mineralized intrusions, *Econ. Geol.,* 2008, vol. 103, pp. 877–908.

Audetat, A., Source and evolution of molybdenum in the porphyry Mo(-Nb) deposit at Cave Peak, Texas, *J. Petrol.,* 2010, vol. 51, pp. 1739–1760.

Audetat, A., Dolejs, D., and Lowenstern, J.B., Molybdenite saturation in silicic magmas: occurrence and petrological implications, *J. Petrol.,* 2011, vol. 52, pp. 891–904.

Baker, T., Ebert, S., Rombach, C., and Ryan, C.G., Chemical compositions of fluid inclusions in intrusion-related gold systems, Alaska and Yukon, using PIXE microanalysis, *Econ. Geol.,* 2006, vol. 101, pp. 311–327.

Baker, T., Mustard, R., Fu, B., et al., Mixed messages in iron–copper–gold systems of the Cloncurry district, Australia: insights from PIXE analysis of halogens and copper in fluid inclusions, *Mineral. Deposita,* 2008, vol. 43, pp. 599–608.

Beaudoin, Y., Scott, S.D., Gorton, M.P., et al., Pb and other ore metals in modem seafloor environments: evidence from melt inclusions, *Mar. Geol.,* 2007, vol. 242, pp. 271–289.

Berlo, K., Tuffen, H., Smith, V.C., et al., Element variations in rhyolitic magma resulting from gas transport, *Geochim. Cosmochim. Acta,* 2013, vol. 121, pp. 436–451.

Beuchat, S., Moritz, R., and Pettke, T., Fluid evolution in the W–Cu–Zn–Pb San Cristobal vein, Peru: fluid inclusion and stable isotope evidence, *Chem. Geol.,* 2004, vol. 210, pp. 201–24.

Bortnikov N.S., Kovalenko V.I., Lykhin D.A. et al., Fundamental principles of the formation of gold and rare-metal resource base of Russia: models of deposits, ore sources, and geodynamic settings, in *Fundamental'nye osnovy formirovaniya resursnoi bazy strategicheskogo syr'ya (Au, Ag, Pt, Cu, redikie elementy i metally* (Fundamental Principles of the Formation of Resource Base of Strategic Raw Material (Au, Ag, Pt, Cu, rare elements and metals), Moscow: GEOS, 2012.

Bortnikov, N.S., Gamyanin, G.N., Vikent'eva, O.V., et al., The Sarylakh and Sentachan gold—antimony deposits, Sakha-Yakutia: a case of combined mesothermal gold—quartz and epithermal stibnite ores, *Geol. Ore Deposits,* 2010, vol. 52, pp. 339–372.

Bouvier, A.-S., Deloule, E., and Metrich, N., Fluid inputs to magma sources of St. Vincent and Grenada (Lesser Antilles): new insights from trace elements in olivine-hosted melt inclusions, *J. Petrol.,* 2010, vol. 51, pp. 1597–1615.

Castillo, P.R., Klein, E., Bender, J., et al., Petrology and Sr, Nd, and Pb isotope geochemistry of mid-ocean ridge basalt glasses from the 11°45′ N to 15°00′ N segment of the East Pacific Rise, *Geochem. Geophys. Geosyst.,* 2000, vol. 1.

Caulfield, J.T., Turner, S.P., Smith, I.E.M., et al., Magma evolution in the primitive, intra-oceanic Tonga arc: petrogenesis of basaltic andesites at Tofua volcano, *J. Petrol.,* 2012, vol. 53, pp. 1197–1230.

Collins, S.J., Pyle, D.M., and Maclennan, J., Melt inclusions track pre-eruption storage and dehydration of magmas at Etna, *Geology,* 2009, vol. 37, pp. 571–574.

Cottrell, E. and Kelley, K.A., The oxidation state of Fe in MORB glasses and the oxygen fugacity of the upper mantle, *Earth Planet. Sci. Lett.,* 2011, vol. 305, pp. 270–82.

Danyushevsky, L.V., Eggins, S.M., Falloon, T.J., and Christie, D.M., H_2O abundance in depleted to moderately enriched mid-ocean ridge magmas. Part I: incompatible behavior, implications for mantle storage, and origin of regional variations, *J. Petrol.,* 2000, vol. 41, pp. 1329–1364.

Devey, C.W., Albarede, F., Cheminee, J.-L., et al., Active submarine volcanism on the society hotspot swell (West Pacific): a geochemical study, *J. Geophys. Res.,* 1990, vol. 95, no. B4, pp. 5049–5066.

Field, L., Blundy, J., Brooker, R.A., et al., Magma storage conditions beneath Dabbahu volcano (Ethiopia) constrained by petrology, seismicity and satellite geodesy, *Bull. Volcanol.,* 2012, vol. 74, pp. 981–1004.

Frey, F.A., Pringle, M., Meleney, P., et al., Diverse mantle sources for Ninetyeast Ridge magmatism: geochemical constraints from basaltic glasses, *Earth Planet. Sci. Lett.,* 2011, vol. 303, pp. 215–224.

Fusswinkel, T., Wagner, T., Wenzel, T., et al., Red bed and basement sourced fluids recorded in hydrothermal Mn-Fe-As veins, Sailauf (Germany): a LA-ICPMS fluid inclusion study, *Chem. Geol.,* 2014, vol. 363, pp. 22–39.

Girnis, A.V., Olivine–orthopyroxene–melt equilibrium as a thermobarometer for mantle-derived magmas, *Petrology,* 2003, vol. 11, pp. 101–113.

Goss, A.R., Perfit, M.R., Ridley, W.I., et al., Geochemistry of lavas from the 2005-2006 eruption at the East Pacific Rise, 9°46′ N–9°56′ N: implications for ridge crest plumbing and dacadal changes in magma chamber compositions, *Geochem. Geophys. Geosyst.,* 2010, vol. 11, no. 5, pp. 1–35.

Gray, T.R., Hanley, J.J., Dostal, J., and Guillong, M., Magmatic enrichment of uranium, thorium, and rare earth elements in Late Paleozoic rhyolites of southern New Brunswick, Canada: evidence from silicate melt inclusions, *Econ. Geol.,* 2011, vol. 106, pp. 127–143.

Gurenko, A.A. and Sobolev, A.V., Crust-primitive magma interaction beneath neovolcanic rift zone of Iceland recorded in gabbro xenoliths from Midfell, SW Iceland, *Contrib. Mineral. Petrol.,* 2006, vol. 151, pp. 495–520.

Guzmics, T., Mitchell, R.H., Szabo, C., et al., Liquid immiscibility between silicate, carbonate and sulfide melts in melt inclusions hosted in co-precipitated minerals from Kerimasi Volcano (Tanzania): evolution of carbonated nephelinitic magma, *Contrib. Mineral. Petrol.,* 2012, vol. 164, pp. 101–122.

Halter, W.E., Heinrich, C.A., and Pettke, T., Laser-ablation ICP-MS analysis of silicate and sulfide melt inclusions in an andesitic complex II: evidence for magma mixing and magma chamber evolution, *Contrib. Mineral. Petrol.,* 2004, vol. 147, pp. 397–412.

Hammer, J.E., Coombs, M.L., Shamberger, P.J., and Kimura, J.-I., Submarine sliver in North Kona: a window into the early magmatic and growth history of Hualalai Volcano, Hawaii, *J. Volcanol. Geotherm. Res.,* 2006, vol. 151, pp. 157–188.

Hammerli, J., Rusk, B., Spandler, C., et al., In situ quantification of Br and Cl in minerals and fluid inclusions by LA-ICP-MS: a powerful tool to identify fluid sources, *Chem. Geol.,* 2013, vol. 337–338, pp. 75–87.

Hanley, J., Ames, D., Barnes, J., et al., Interaction of magmatic fluids and silicate melt residues with saline groundwater in the footwall of the Sudbury igneous complex, Ontario, Canada: new evidence from bulk rock geochemistry, fluid inclusions and stable isotopes, *Chem. Geol.,* 2011, vol. 281, pp. 1–25.

Hawkins, J.W., Lonsdale, P.F., Macdougall, J.D., and Volpe, A.M., Petrology of the axial ridge of the Mariana trough back-arc spreading center, *Earth Planet. Sci. Lett.,* 1990, vol. 100, pp. 226–250.

Hedenquist, J.W. and Lowenstern, J.B., The role of magmas in the formation of hydrothermal ore deposits, *Nature,* 1994, vol. 370, pp. 519–527.

Holwell, D.A., McDonald, I., and Butler, I.B., Precious metal enrichment in the platreef, Bushveld Complex, South Africa: evidence from homogenized magmatic sulfide melt inclusions, *Contrib. Mineral. Petrol.,* 2011, vol. 161, pp. 1011–1026.

Hurtic, N.C., Heinrich, C.A., Driesner, Y., et al., Fluid evolution and uranium (-Mo-F) mineralization at the

Maureen Deposit (Queensland, Australia): unconformity-related hydrothermal ore formation with a source in the volcanic cover sequence, *Econ. Geol.,* 2014, vol. 109, pp. 737–773.

Jenner, F.E., O'Neill, H.St.C., Arculus, R.J., and Mavrogenes, J.A., The magnetite crisis in the evolution of arc-related magmas and the initial concentration of Au, Ag and Cu, *J. Petrol.,* 2010, vol. 51, pp. 2445–2464.

Jenner, F.E. and O'Neill, H.Sr.C., Analysis of 60 elements in 616 ocean floor basaltic glasses, *Geochem. Geophys. Geosyst.,* 2012, vol. 13, pp. 1–11.

Jenner, F.E., Arculus, R.J., Mavrogenes, J.A., et al., Chalcophile element systematics in volcanic glasses from the northwestern Lau Basin, *Geochem. Geophys. Geosyst.,* 2012, vol. 13, no. 6, pp. 1–25.

Johnson, E.R., Kamenetsky, V.S., and McPhie, J., The behavior of metals (Pb, Zn, As, Mo, Cu) during crystallization and degassing of rhyolites from the Okataina volcanic center, Taupo volcanic zone, New Zealand, *J. Petrol.,* 2013, vol. 54, pp. 1641–1659.

Jordan, B.R., Sigurdsson, H., Carey, S.N., et al., Geochemical variation along and across the Central American Miocene paleoarc in Honduras and Nicaragua, *Geochim. Cosmochim. Acta,* 2007, vol. 71, pp. 3581–3591.

Kamenetsky, V.S. and Eggins, S.M., Systematics of metals, metalloids, and volatiles in MORB melts: effects of partial melting, crystal fractionation and degassing (a case study of Macquarie island glasses), *Chem. Geol.,* 2012, vol. 302-303, pp. 76–86.

Klemm, L.M., Pettke, T., Heinrich, C.A., and Campos, E., Hydrothermal evolution of the El Teniente deposit, Chile: porphyry Cu–Mo ore deposition from low-salinity magmatic fluids, *Econ. Geol.,* 2007, vol. 102, pp. 1021–1045.

Konig, S., Munker, C., Hohl, S., et al., The Earth's tungsten budget during mantle melting and crust formation, *Geochim. Cosmochim. Acta,* 2011, vol. 75, pp. 2119–2136.

Kotzeva, B.G., Guillong, M., Stefanova, E., and Piperov, N.B., LA-ICP-MS analysis of single fluid inclusions in a quartz crystal (Madan ore district, Bulgaria), *J. Geochem. Explor.,* 2011, vol. 108, pp. 163–175.

Kouzmanov, K., Pettke, T., and Heinrich, C., Direct analysis of ore-precipitating fluids: combined IR microscopy and LA-ICP-MS study of fluid inclusions in opaque ore minerals, *Econ. Geol.,* 2010, vol. 105, pp. 351–373.

Kovalenker, V.A., Conditions of formation and factors of large-scale gold accumulation in porphyritic and epithermal deposits, in *Krupnye i superkrupnye mestorozhdeniya rudnykh poleznykh iskopaemykh (Large and Superlarge Ore Deposits)*, Moscow: IGEM RAN, 2006, vol. 2, pp. 143–214.

Kovalenko, V.I., Naumov, V.B., Girnis, A.V., et al., Average compositions of magmas and mantle sources of mid-ocean ridges and intraplate oceanic and continental settings estimated from the data on melt inclusions and quenched glasses of basalts, *Petrology,* 2007, vol. 15, pp. 335–368.

Kurosawa, M., Ishi, S., and Sasa, K., Trace-element compositions of single fluid inclusions in the Kofu granite, Japan: implications for compositions of granite-derived fluids, *Island Arc,* 2010, vol. 19, pp. 40–59.

Lang, J.L. and Baker, T., Intrusion-related gold systems: the present level of understanding, *Mineral. Deposita,* 2001, vol. 36, pp. 477–489.

Laubier, M., Gale, A., and Langmuir, C.H., Melting and crustal processes at the famous segment (Mid-Atlantic Ridge): new insights from olivine-hosted melt inclusions from multiple samples, *J. Petrol.,* 2012, vol. 53, pp. 665–698.

Le Fort, D., Hanley, J., and Guillong, M., Subepithermal au–pd mineralization associated with an alkalic porphyry Cu–Au deposit, Mount Milligan, Quesnel terrane, British Columbia, Canada, *Econ. Geol.,* 2011, vol. 106, pp. 781–808.

Leisen, M., Dubessy, J., Boiron, M.-C., and Lach, P., Improvement of the determination of element concentrations in quartz-hosted fluid inclusions by LA-ICP-MS and Pitzer thermodynamic modeling of ice melting temperature, *Geochim. Cosmochim. Acta,* 2012, vol. 90, pp. 110–125.

Lerchbaumer, L. and Audetat, A., The metal content of silicate melts and aqueous fluids in subeconomically Mo mineralized granites: implications for porphyry Mo genesis, *Econ. Geol.,* 2013, vol. 108, pp. 987–1013.

Li, N., Ulrich, T., Chen, Y.J., et al., Fluid evolution of the Yuchiling porphyry Mo deposit, East Qinling, China, *Ore Geol. Rev.,* 2012, vol. 48, pp. 442–459.

Liu, Y., Anderson, A.T., Wilson, C.J.N., et al., Mixing and differentiation in the Oruanui rhyolitic magma, Taupo, New Zealand: evidence from volatiles and trace elements in melt inclusions, *Contrib. Mineral. Petrol.,* 2006, vol. 151, pp. 71–87.

Luders, V., Romer, R.L., Gilg, H.A., et al., A geochemical study of the Sweet Home Mine, Colorado mineral belt, USA: hydrothermal fluid evolution above a hypothesized granite cupola, *Mineral. Deposita,* 2009, vol. 44, pp. 415–434.

MacLennan, J. Concurrent mixing and cooling of melts under Iceland, *J. Petrol.,* 2008. V. 49. P. 1931–1953.

Mao, J., Pirajno, F., Lehmann, B., et al., Distribution of porphyry deposits in the Eurasian continent and their corresponding tectonic settings, *J. Asia Earth Sci.,* 2014, vol. 79, pp. 576–584.

Marsala, R., Wagner, T., and Walle, M., Late-metamorphic veins record deep ingression of meteoric water: a LA-ICPMS fluid inclusion study from the fold-and-thrust belt of the Rhenish Massif, Germany, *Chem. Geol.,* 2013, vol. 351, pp. 134–153.

McPhie, J., Kamenetsky, V., Allen, S., et al., The fluorine link between a supergiant ore deposit and a silicic large igneous province, *Geology,* 2011, vol. 39, pp. 1003–1006.

Meinert, L.D., Hedenquist, J.W., Saton, H., and Matsuhisa, Y., Formation of anhydrous and hydrous skarn in Cu–Au ore deposits by magmatic fluids, *Econ. Geol.,* 2003, vol. 98, pp. 147–156.

Metrich, N., Zanon, V., Creon, L., et al., Is the "Azores" "hotspot" a wetspot? Insights from the geochemistry of fluid and melt inclusions in olivine of Pico Basalts, *J. Petrol.,* 2014, vol. 55, pp. 377–393.

Miron, G.D., Wagner, T., Walle, M., and Heinrich, C.A., Major and trace-element composition and pressure-temperature evolution of rock-buffered fluids in low-grade accretionary-wedge metasediments, Central Alps, *Contrib. Mineral. Petrol.,* 2013, vol. 165, pp. 981–1008.

Muller, D. and Forrestal, P., The shoshonite porphyry Cu–Au association at Bajo de La Alumbdrera, Catamarca Province, Argentina, *Mineral. Petrol.* 1998, vol. 64, pp. 47–64.

Mungall, J.E., Roasting the mantle: slab melting and the genesis of major Au and Au-rich Cu deposits, *Geology,* 2002, vol. 30, pp. 915–918.

Mustard, R., Ulrich, T., Kamenetsky, V., and Mernagh, T., Gold and metal enrichment in natural granitic melts during fractional crystallization, *Geology,* 2006, vol. 34, pp. 85–88.

Nadeau, O., Stix, J., and Williams-Jones, A.E., The behavior of Cu, Zn and Pb during magmatic-hydrothermal activity at Merapi volcano, Indonesia, *Chem. Geol.,* 2013, vol. 342, pp. 167–179.

Naumov, V.B., Kovalenko, V.I., Dorofeeva, V.A., and Yarmolyuk, V.V., Average concentrations of major, volatile, and trace elements in magmas of various geodynamic settings, *Geochem. Int.,* 2004, vol. 42, no. 10, pp. 977–987.

Naumov, V.B., Kovalenko, V.I., Dorofeeva, V.A., et al., Average compositions of igneous melts from main geodynamic settings according to the investigation of melt inclusions in minerals and quenched glasses of rocks, *Geochem. Int.,* 2010, vol. 48, no. 12, pp. 1185–1207.

Naumov, V.B., Dorofeeva, V.A., Girnis, A.V., and Yarmolyuk, V.V., Comparison of major, volatile, and trace element contents in the melts of mid-ocean ridges on the basis of data on inclusions in minerals and quenched glasses of rocks, *Geochem. Int.,* 2014, vol. 52, no. 5, pp. 347–364.

Neave, D.A., Fabbro, G., Herd, R.A., et al., Melting, differentiation and degassing at the Pantelleria volcano, Italy, *J. Petrol.,* 2012, vol. 53, pp. 637–663.

Nikogosian, I.K., Bergen van, M.J., Heterogeneous mantle sources of patassium-rich magmas in Central-Southern Italy: melt inclusion evidence from Roccamonfina and Ernici (Mid Latina Valley), *J. Volcanol. Geotherm. Res.,* 2010, vol. 197, pp. 279–302.

Niu, Y., Waggoner, D.G., Sinton, J.M., and Mahoney, J.J., Mantle source heterogeneity and melting processes beneath seafloor centers: the East Pacific Rise, 18°–19° S, *J. Geophys. Res.,* 1996, vol. 101, no. B12, pp. 27711–27733.

Niu, Y. and Batiza, R., Trace element evidence from seamounts for recycled oceanic crust in the Eastern Pacific mantle, *Earth Planet. Sci. Lett.,* 1997, vol. 148, pp. 471–483.

Palme, H. and O'Neill, H.St.C., Cosmochemical estimates of mantle composition, in *Treatise on geochemistry,* Amsterdam: Elsevier, 2003, vol. 2.

Perugini, D. and Poli, G., Analysis and numerical simulation of chaotic advection and chemical diffusion during magma mixing: petrological implications, *Lithos,* 2004, vol. 78, pp. 43–66.

Pettke, T., Oberli, F., Audetat, A., et al., Recent developments in element concentration and isotope ratio analysis of individual fluid inclusions by laser ablation single and multiple collector ICP-MS, *Ore Geol. Rev,* 2012, vol. 44, pp. 10–38.

Pritchard, C.J. and Larson, P.B., Genesis of post-caldera eastern upper basin member rhyolites, Yellowstone, WY: from volcanic stratigraphy, geochemistry, and radiogenic isotope modeling, *Contrib. Mineral. Petrol.,* 2012, vol. 164, pp. 205–228.

Pudack, C., Halter, W.E., Heinrich, C.A., and Pettke, T., Evolution of magmatic vapor to gold-rich epithermal liquid: the porphyry to epithermal transition at Navados de Famatina, northwest Argentina, *Econ. Geol.,* 2009, vol. 104, pp. 449–477.

Ren, Z-Y., Ingle, S., Takahashi, E., et al., The chemical structure of the Hawaiian mantle plume, *Nature,* 2005, vol. 436, pp. 837–840.

Richard, A., Rozsypal, C., Mercadier, J., et al., Giant uranium deposits formed from exceptionally uranium-rich acidic brines, *Nature Geosci.,* 2012, vol. 5, pp. 142–146.

Richards, J.P., Tectono-magmatic precursors for porphyry Cu–(Mo–Au) deposit formation, *Econ. Geol.,* 2003, vol. 98, pp. 1515–1533.

Rickers, K., Thomas, R., and Heinrich, W., The behavior of trace elements during the chemical evolution of the H_2O-, B-, and F-rich granite-pegmatite-hydrothermal system at Ehrenfriedersdorf, Germany: a SXRF study of melt and fluid inclusions, *Mineral. Deposita,* 2006, vol. 41, pp. 229–245.

Robertson, K., Simon, A., Pettke, T., et al., Melt inclusion evidence for magma evolution at Mutnovsky Volcano, *Geofluids,* 2013, vol. 13, pp. 421–439.

Rosenbaum, J.M., Zindler, A., and Rubenstone, J.L., Mantle fluids: evidence from fluid inclusions, *Geochim. Cosmochim. Acta,* 1996, vol. 60, pp. 3229–3252.

Rowe, M.C., Kent, A.J.R., and Nielsen, R.L., Subduction influence on oxygen fugacity and trace and volatile elements in basalts across the Cascade Volcanic Arc, *J. Petrol.,* 2009, vol. 50, pp. 61–91.

Ruscitto, D.M., Wallace, P.J., Johnson, E.R., et al., Volatile contents of mafic magmas from cinder cones in the Central Oregon High Cascades: implications for magma formation and mantle conditions in a hot arc, *Earth Planet. Sci. Lett.,* 2010, vol. 298, pp. 153–161.

Rusk, B.G., Reed, M.H., Dilles, J.H., et al., Compositions of magmatic hydrothermal fluids determined by LA-ICP-MS of fluid inclusions from the porphyry Copper–Molybdenum deposit at Butte, MT, *Chem. Geol.,* 2004, vol. 210, pp. 173–199.

Sadofsky, S.J., Portnyagin, M., Hoernle, K., and Bogaard, P., Subduction cycling of volatiles and trace elements through the Central American volcanic arc: evidence from melt inclusions, *Contrib. Mineral. Petrol.,* 2008, vol. 155, pp. 433–456.

Safonov, Yu.G., Popov, V.V., Volkov, A.V., and Gongal'skii, B.I., Geodynamic and geotectonic settings of the formation of large gold concentrations, in *Krupnye i superkrupnye mestorozhdeniya rudnykh poleznykh iskopaemykh (Large and Superlarge Ore Deposits)*, Moscow: IGEM RAN, 2006, vol. 2, pp. 97–142.

Salisbury, M.J., Patton, J.R., Kent, A.J.R., et al., Deep-sea ash layers reveal evidence for large, Late Pleistocene and Holocene explosive activity from Sumatra, Indonesia, *J. Volcanol. Geotherm. Res.,* 2012, vol. 231-232, pp. 61–71.

Saunders, K.E., Baker, J.A., and Wysoczanski, R.J., Microanalysis of large silicic magma in continental and oceanic arcs: melt inclusions in Taupo volcanic zone and Kermadec arc rocks, South West Pacific, *J. Volcanol. Geotherm. Res.,* 2010, vol. 190, pp. 203–218.

Sawkins, F.J., *Metal deposits in relation to plate tectonics, Minerals and Rocks,* 1990, vol. 17.

Seo, J.H., Guillong, M., and Heinrich, C.A., Separation of molybdenum and copper in porphyry deposits: the roles of sulfur, redox, and pH in ore mineral deposition at Bingham Canyon, *Econ. Geol.,* 2012, vol. 107, pp. 333–356.

Silantyev, S.A., Danyushevskii, L.V., Plechova, A.A., et al., "Geochemical and isotopic signatures of magmatic products in the MAR rift valley at 12°49′–17°23′ N and 29°59′–33°41′ N: evidence of two contrasting sources of the parental melts, *Petrology,* 2008, vol. 16, pp. 36–62.

Sillitoe, R.H., Relation of metal provinces in western America to subduction of oceanic lithosphere, *Geology,* 1972, vol. 83, pp. 813–818.

Sillitoe, R.H., Characteristics and controls of the largest porphyry copper-gold and epithermal gold deposits in the Circum-Pacific region, *Aust. J. Earth Sci.,* 1997, vol. 44, pp. 373–388.

Sillitoe, R. and Hedenquist, J., Linkages between volcanotectonic settings, ore-fluid compositions, and epithermal precious metal deposits, *SEG Spec. Publ.*, 2003, vol. 10, pp. 315–343.

Silva, R.C.F., Hagemann, S., Lobato, L.M., et al., Hydrothermal fluid processes and evolution of the giant Serra Norte jaspilite-hosted iron ore deposits, Carajas mineral province, Brazil, *Econ. Geol.,* 2013, vol. 108, pp. 739–779.

Simonov, V.A., Kovyazin, S.V., Peive, A.A., and Kolmogorov, Yu.P., Geochemical characteristics of magmatic systems in the region of the Sierra Leone Fracture Zone, Central Atlantic: evidence from melt inclusions, *Geochem. Int.,* 2005, vol. 43, no. 7, pp. 682–693.

Sirbescu, M.L., Krukowski, E.G., Schmidt, C., et al., Analysis of boron in fluid inclusions by microthermometry, laser ablation ICP-MS, and Raman spectroscopy: application to the Cryo-Genie pegmatite, San Diego County, California, USA, *Chem. Geol.,* 2013, vol. 342, pp. 138–150.

Sisson, T.W., Kimura, J.-I., and Coombs, M.L., Basanite–nephelinite suite from early Kilauea: carbonated melts of phlogopite–garnet peridotite at Hawaii's leading magmatic edge, *Contrib. Mineral. Petrol.,* 2009, vol. 158, pp. 803–829.

Slater, L., McKenzie, D., Gronvold, K., and Shimizu, N., Melt generation and movement beneath Theistareykir, NE Iceland, *J. Petrol.,* 2001, vol. 42, pp. C. 321–354.

Sobolev, A.V., Hofmann, A.W., Jochum, K.P., et al., A young source for the Hawaiian plume, *Nature,* 2011, vol. 476, pp. 434–437.

Stoffell, B., Wilkinson, J.J., and Jeffries, T.E., Metal transport and deposition in hydrothermal veins revealed by 213 nm UV laser ablation microanalysis of single fluid inclusions, *Am. J. Sci.,* 2004, vol. 304, pp. 533–557.

Stoffell, B., Appold, M.S., Wilkinson, J.J., et al., Geochemistry and evolution of Mississippi valley-type mineralizing brines from the Tri-State and Northern Arkansas districts determined by LA-ICP-MS microanalysis of fluid inclusions, *Econ. Geol.,* 2008, vol. 103, pp. 1411–1433.

Student, J.J. and Bodnar, R.J., Silicate melt inclusions in porphyry copper deposits: identification and homogenization behavior, *Can. Mineral.,* 2004, vol. 41, pp. 1583–1599.

Su, W., Heinrich, C.A., Pettke, T., et al., Sediment-hosted gold deposits in Guizhou, China: products of wall-rock sulfidation by deep crustal fluids, *Econ. Geol.,* 2009, vol. 104, pp. 73–93.

Sun, W., Bennett, V.C., Eggins, S.M., et al., Rhenium systematics in submarine MORB and back-arc basin glasses: laser ablation ICP-MS results, *Chem. Geol.,* 2003, vol. 196, pp. 259–281.

Sun, W., Bennett, V.C., and Kamenetsky, V.S., The mechanism of re enrichment in arc magmas: evidence from Lau Basin glasses and primitive melt inclusions, *Earth Planet. Sci. Lett.,* 2004, vol. 222, pp. 101–114.

Sun, W.D., Binns, R.A., Fan, A.C., et al., Chlorine in submarine volcanic glasses from the Eastern Manus Basin, *Geochim. Cosmochim. Acta,* 2007, vol. 71, pp. 1542–1552.

Sun, W., Hu, Y., Kamenetsky, V.S., et al., Constancy of Nb/U in the mantle revisited, *Geochim. Cosmochim. Acta,* 2008, vol. 72, pp. 3542–3549.

Sushchevskaya, N.M., Bonatti, E., Peive, A.A., et al., Heterogeneity of rift magmatism in the equatorial province of the Mid-Atlantic Ridge (15° N to 3° S), *Geochem. Int.,* 2002, vol. 40, no. 1, pp. 26–50.

Sushchevskaya, N.M., Kamenetsky, V.S., Murav'ev, K.G., et al., Tholeiitic magmas within the Mid-Atlantic Ridge segments at 25°–30° N: composition, generation conditions, and relation to modern ore formation, *Geochem. Int.,* 2000, vol. 38, no. Suppl. 1, S3–S19.

Thebaud, N., Philippot, P., Rey, P., and Cauzid, J., Composition and origin of fluids associated with lode gold deposits in a Mesoarchean greenstone belt (Warrawoona syncline, Pilbara Craton, Western Australia) using synchrotron radiation X-ray fluorescence, *Contrib. Mineral. Petrol.,* 2006, vol. 152, pp. 485–503.

Timm, C., de Ronde, C.E.J., Leybourne, M.I., et al., Sources of chalcophile and siderophile elements in Kermadec arc lavas, *Econ. Geol.,* 2012, vol. 107, pp. 1527–1538.

Tomkins, A.G. and Mavrogenes, J.A., Generation of metal-rich felsic magmas during crustal anatexis, *Geology,* 2003, vol. 31, pp. 765–768.

Tomkins, A.G., Weinberg, R.F., and McFarlane, C.R.M., Preferential magma extraction from K- and metal-enriched source regions in the crust, *Mineral. Deposita,* 2009, vol. 44, pp. 171–181.

Ulrich, T., Gunther, D., and Heinrich, C., The evolution of porphyry Cu–Au deposit, based on LA-ICP-MS analysis of fluid inclusions: Bajo de La Alumbrera, Argentina, *Econ. Geol.,* 2001, vol. 96, pp. 1743–1774.

Vanko, D.A., Bonnin-Mosbah, M., Philippot, P., et al., Fluid inclusions in quartz from oceanic hydrothermal specimens and the Bingham, Utah porphyry-Cu deposit: a study with PIXE and SXRF, *Chem. Geol.,* 2001, vol. 173, pp. 227–238.

Vlastelic, I., Menard, G., Gannoun, A., et al., Magma degassing during the April 2007 collapse of Piton de La Fournaise: the record of semi-volatile trace elements (Li, B, Cu, In, Sn, Cd, Re, Tl, Bi), *J. Volcanol. Geotherm. Res.,* 2013, vol. 254, pp. 94–107.

Volkov, A.V., Sidorov, A.A., and Starostin, V.I., *Metallogeniya vulkanogennykh poyasov i zon aktivizatsii (Metallogeny of Volcanogenic Belts and Actovation Zones)*, Moscow: MAKS Press, 2014.

Wallace, P.J., Anderson, A.T., and Davis, A.M., Gradients in H_2O, CO_2, and exsolved gas in a large-volume silicic magma system: interpreting the record preserved in melt inclusions from the Bishop tuff, *J. Geophys. Res.,* 1999, vol. 104, no. B9, pp. 20097–20122.

Wallier, S., Rey, R., Kouzmanov, K., et al., Magmatic fluids in the breccia-hosted epithermal Au–Ag deposit of Rosia Montana, Romania, *Econ. Geol.,* 2006, vol. 101, pp. 923–954.

Waters, C.L., Sims, K.W.W., Perfit, M.R., et al., Perspective on the genesis of E-MORB from chemical and isotopic heterogeneity at 9°–10° N East Pacific Rise, *J. Petrol.,* 2011, vol. 52, pp. 565–602.

Webster, J.D. and Duffield, W.A., Extreme halogen abundances in tin-rich magma of the Taylor Creek rhyolite, New Mexico, *Econ. Geol.,* 1994, vol. 89, pp. 840–850.

Webster, J.D., Burt, D.M., and Aguillon, R.A., Volatile and lithophile trace-element geochemistry of Mexican tin rhyolite magmas deduced from melt inclusions, *Geochim. Cosmochim. Acta,* 1996, vol. 60, pp. 3267–3283.

Wehrmann, H., Hoernle, K., Portnyagin, M., et al., Volcanic CO_2 output at the Central American subduction zone inferred from melt inclusions in olivine crystals from mafic tephras, *Geochem. Geophys. Geosyst.,* 2011, vol. 12, no. 6, pp. 1–16.

Wilkinson, J.J., Stoffell, B., Wilkinson, C.C., et al., Anomalously metal-rich fluids form hydrothermal ore deposits, *Science,* 2009, vol. 323, pp. 764–767.

Workman, R.K., Hart, S.R., Jackson, M., et al., Recycled metasomatized lithosphere as the origin of the enriched mantle II (EM2) end-member: evidence from the Samoan volcanic chain, *Geochem. Geophys. Geosyst.,* 2004, vol. 5, no. 4, pp. 1–44.

Zajacz, Z. and Halter, W., LA-ICPMS analyses of silicate melt inclusions in co-precipitated minerals: quantification, data analysis and mineral/melt partitioning, *Geochim. Cosmochim. Acta,* 2007, vol. 71, pp. 1021–1040.

Zaw, K., Hunns, S.R., Large, R.R., et al., Microthermometry and chemical composition of fluid inclusions from the Mt Chalmers volcanic-hosted massive sulfide deposits, Central Queensland, Australia: implications for ore genesis, *Chem. Geol.,* 2003, vol. 194, pp. 225–244.

Zedgenizov, D.A., Rege, S., Griffin, W.L., et al., Composition of trapped fluids in cuboid fibrous diamonds from the Udachnaya kimberlite: LAM-ICP-MS analysis, *Chem. Geol.,* 2007, vol. 240, pp. 151–162.

Zhao, Z., Xiong, X., Wang, Q., et al., Alkali-rich igneous rocks and related Au and Cu large and superlarge deposits in China, *Science in China. Ser. D,* 2003, vol. 46, pp. 1–13.

Translated by V. Popov